AN EXPERIMENTAL MICROMECHANICAL – FINITE ELEMENT ASSISTED –APPROACH INTO THE COMPRESSIVE FAILURE MECHANISMS OF CARBON FIBRE COMPOSITES

S. Goutianos[1,2], T. Peijs[2], C. Galiotis[1,2,3]

[1]Institute of Chemical Engineering and High Temperature Chemical Processes, Foundation of Research and Technology—Hellas, P.O. Box 1414, Patras 265 00, Greece
[2]Materials Department, Queen Mary University of London, Mile End Road, London E1 4NS, UK
[3]Department of Materials Science, University of Patras, 26504, Patras, Greece

ABSTRACT

Understanding the microscopic mechanical behaviour of carbon fibre composites is essential in the analysis of the compressive response of unidirectional carbon fibre composites. Many analytical models have been proposed to predict the compressive strength of this class of materials, which combined with the experimental data existing in the literature, provide a relatively good understanding of this topic. Some fundamental issues, however, still remain open, such as the effect of a compressive fibre break or discontinuity on its surrounding intact fibres, or the effect of fibre/matrix interfacial properties. The present paper is an attempt to highlight the aspect of compression by employing multi-fibre model geometries. Then the FE method is used to validate/interpret the experimental results. The experimental and numerical findings suggest that compressive failure of high modulus carbon fibre/epoxy unidirectional composites is mainly controlled by the compressive response of the carbon fibres themselves.

1. INTRODUCTION

The compressive failure of unidirectional fibre composites is typically 60%-70% of their tensile strength, which is of major concern since there are many applications in which such materials are subjected to high compressive stresses [1]. As a result, the compressive behaviour of these materials has received significant attention in recent years; a better understanding of the phenomena involved in compressive failure is a basis for fully exploiting this class of materials.

Early investigations associated compressive failure with a fibre buckling process in an elastic matrix [2-3]. However, predictions were 3-4 times higher that the measured values, even when the initial assumptions were extended to account i.e. for matrix non-linear constitutive behaviour. On the other hand, Budiansky [4] recognised the importance of initial fibre waviness and that of matrix or composite shear yield strength as the main factors controlling the compressive strength. It is now widely established that this failure mechanism (plastic microbuckling of the fibres in the inelastic matrix) is the most important in composite materials loaded in compression. This failure mode is facilitated by the presence of regions where the fibres are misoriented with respect to the loading axis (polymeric matrices have relatively low yield stress and under compression a misalignment of the order of a few degrees can cause matrix yielding). This results in microbuckling and failure due to loss of stiffness. In general these models have given fairly good quantitative agreement between predictions and experimental findings, although it should be mentioned that there is usually a large degree of uncertainty concerning the fibre misalignment in a composite. More importantly, these analyses fail to capture the physics of the problem i.e. predicting realistic kink band angles.

As a consequence, alternative theories have been developed, which consider the possibility of the failure behaviour being controlled by the compressive failure of the fibres themselves. Kozey [5] concluded that stress raisers have an important effect. This is well demonstrated in the work of Lankford [6] who showed that a cluster of broken fibres forms a defect zone, which in turn leads to kink band formation. Moreover, he suggested that these initial fibre breaks would lie along parallel shear bands rather than normal to the reinforcement direction.

Narayanan and Schadler [7] expanded Lankford's ideas and have used the Laser Raman Spectroscopy technique to study kink band initiation in carbon-epoxy composites. In agreement with Lankford's work, they suggested that once the damage zone, consisting of broken and/or crushed fibres, reaches a critical size, local instability causes microbuckling. Recently, Garland et al [8] developed a simple shear-lag model to calculate the stress state around broken fibres, which has been used to predict the formation of damage zones.
As it becomes evident, the issue of compression appears to be more complicated than generally appreciated. Further experimental/analytical work is needed for the complete description of the compressive behaviour. In the current work Raman spectroscopy is used to assess the stress transfer efficiency in compression of single-(high modulus carbon) fibre discontinuous model geometries. The FE method is also employed to further examine the compressive failure these single-fibre model composites. Then, the compressive response of multi-fibre composites is investigated as an attempt to build a bridge between the response of one and multi-fibre composites.

2. EXPERIMENTAL

2.1 MATERIALS & SPECIMEN PREPARATION

Surface treated high-modulus carbon fibres (M40-40B) were used. These fibres have a longitudinal Young's modulus of 390 GPa and an effective diameter of 6.6 μm (the fibre properties are listed in Table 1). The fibres were embedded in a two component system: Epikote 828/Ankamine 1628 (Shell). The matrix properties are given also in Table 1.
Two different specimen geometries have been employed; a) a single and b) a bundle of fibres embedded in an epoxy matrix. In both cases the fibres were aligned to the loading axis. The prism length was twice its width/thickness to avoid macrobuckling of the specimen according to ASTM 695 standards. Care was taken to embed the fibres at a distance away from the surface. The composite coupons were then cured at room temperature for one week. A low curing temperature was preferred in order to eliminate the development of residual stresses on the embedded fibres. The local fibre volume fraction (in the bundle of fibres) was about 55%, whereas the misorientation angle of the fibres with respect to the loading axis was about 2-3^{o}.

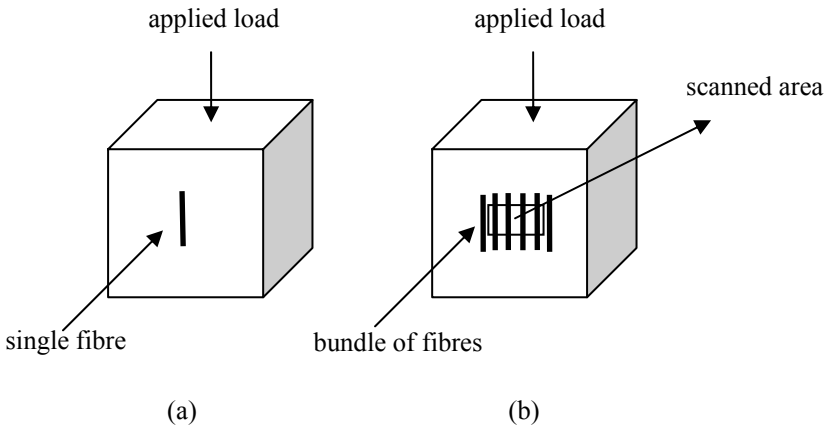

Fig. 1. Geometry of model composites: a) a single, and b) a bundle of fibres embedded in an epoxy matrix.

2.2 SPECIMEN TESTING & RAMAN SPECTRA ACQUISITION

Raman spectra were taken with a Remote Raman Microprobe. The laser used was a 514.5 nm argon ion laser. An incident power of 1.2mW and an exposure time of 60 s were chosen in order to avoid fibre overheating. The spatial resolution was 2μm. The spectra characteristics, i.e. peak positions were derived by fitting the raw data with Lorentzian distribution functions. Fig. 2 shows schematically the experimental set-up used.

The shift of the Raman wavenumber of the carbon fibres upon the application of a tensile or compressive strain was measured with the cantilever beam test. This was done by attaching individual filaments on the top surface of a specially made cantilever beam, which can be flexed up or down subjecting the fibres to compression or tension, respectively.

Table 1

Mechanical properties of fibre and resin

Mechanical parameters	Carbon fibre	Epoxy matrix
E_1 (GPa)	390	2
E_2 (GPa)	20	2
ν_{12} (-)	0.03	0.3
G_{12} (GPa)	12	0.77
G_{13} (GPa)	5	0.77
G_{23} (GPa)	12	0.77

E: Young's modulus, G: shear modulus, v: Poisson's ratio, 1: longitudinal direction, 2: transverse direction, 3: out of plane direction.

The second order peak of the carbon fibre, at 2760cm^{-1}, was employed for fibre strain measurements. The Raman wavenumber shift versus fibre strain is shown in Fig. 3. The experimental data were fitted with a polynomial function. As it can be seen the M40-40B carbon fibre fails at a strain of approximately 1% in tension, whereas its compressive failure strain is only about -0.6%. More importantly, it can be observed that even high-modulus carbon fibres display a strongly non-linear behaviour in compression with the linear part to extend up to a strain of -0.35% approximately.

The multi short-fibre specimens were strained at distinct levels up to –0.9%. The applied strain rate, used for the transition from one strain level to the next one, was 4.2 10^{-5} s^{-1}. Point by point Raman measurements were taken at each strain level. The applied strain on the specimens was also monitored by two strain gauges, attached to the resin surface (on opposite sides) to detect any possible macrobuckling on the specimens.

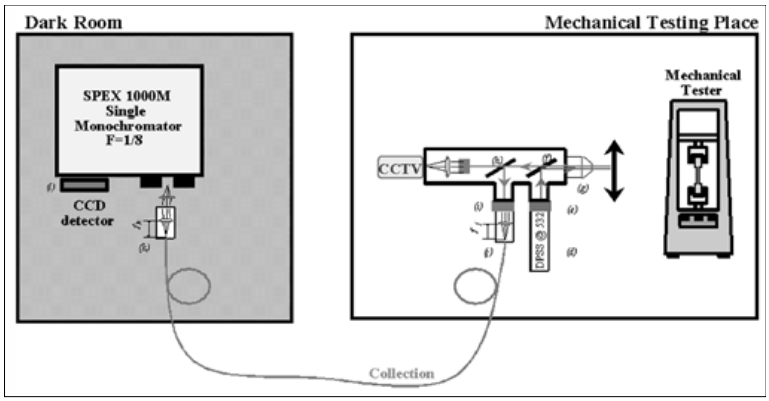

Fig. 2. Remote laser Raman experimental set-up.

Additionally to the mapping of compressive strain in selected fibres within the bundle of fibres a statistical approach was also pursued for monitoring the mechanisms of failure in these composites.

This is based on the indiscriminate point-by-point measurement of fibre strains within a 'large' window of observation without attempting a detailed mapping of the area near a discontinuity i.e. a fibre end. The values of fibre strain collected this way form a distribution. Its peak should provide information on the average strain that the fibres support, whereas its spread is indicative of the extent of 'failure' within the examined specimen volume.

The fibre strain mapping was performed at some distance from the fibre ends in order to avoid end effects. Raman spectra were taken from 200 points, at each applied strain level, within a pre-defined region in the bundle (see Fig. 1(b)).

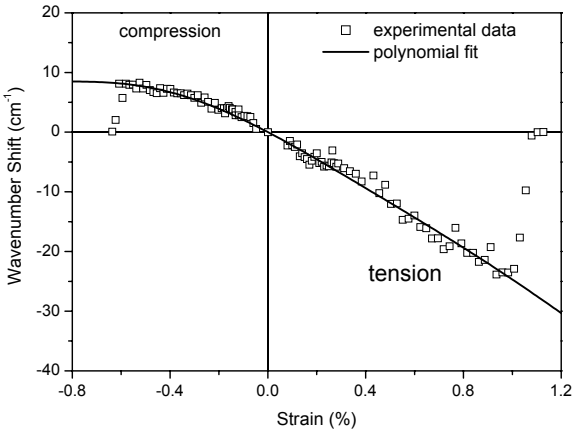

Fig. 3. Raman wavenumber shift versus strain for the M40-40B carbon fibre.

3. FE MODELLING

In has been shown that in the vicinity of a compressive fibre fracture the interface integrity cannot be evaluated from the Raman data [9]. To overcome this problem, a quasi-static plane strain multi-contact non-linear finite element model is employed (see Fig. 4). Secondly, the effect of a compressive fibre break in its adjacent fibres is examined. The FE model is consisting now of an array of fibres).

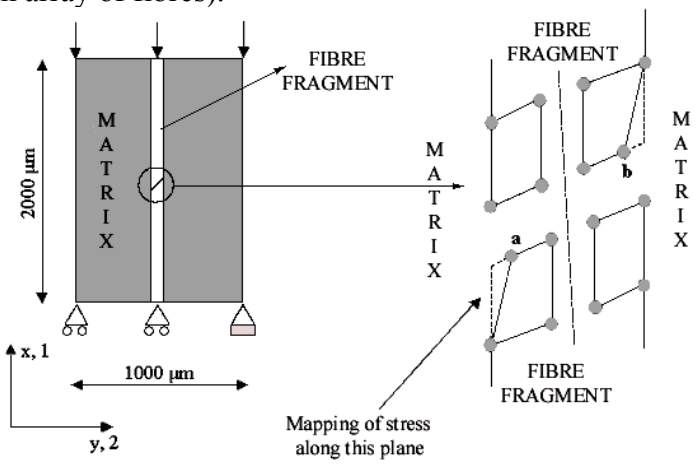

Fig. 4. Schematic representation of the FE model used.

We have chosen to model the fibre fracture problem as a plane stress problem. Fibre fracture is assumed to occur in the centre of the model composite. The fibre is then divided in two fragments, which are fully bonded up to a certain applied strain level (equal to the fibre failure strain experimentally determined in similar specimens. The angle between the fibre fragments is 45^0, equal to the value observed in the experiments [9]. In the subsequent step of the analysis the coefficient of friction between the fibre fragments is reduced allowing in that way the fibre fragments to slide past each other. The fibre fragments (near the fracture site) are also fully bonded to the surrounding matrix. The fibre close to the contact area was modelled using incompatible modes elements in order to prevent shear locking or hourglass effects. The fibre fragments far from the contact area (fibre fracture site) and the matrix material were modelled using full integration elements. Finally, in order to facilitate the multi-contact definition, node *a* and *b* belonging to the fibre fragments were slightly moved as it can be

seen in Fig. 4. This kind of local imperfection results in stress discontinuities at applied strains even much lower than the strain level at which the fibre fragments are allowed to slide past each other. However, this imperfection has minor effects in the overall analysis. The axial fibre stress is calculated at the right hand side of the fibre as it is shown in Fig. 4, whereas the interfacial shear and transverse stresses are calculated at the corresponding fibre/matrix interface.

4. RESULTS & DISCUSSION

Fig. 5 shows the FEA predictions of the axial fibre stress profile in the vicinity of a compressive fibre break (single-fibre model composite). The applied strain is -0.55% where fibre fracture was experimentally observed. It can be seen that for a coefficient of friction of 0.4 the numerical data agrees relatively well with the experimental values (Raman spectroscopy), except at $x \cong 0$ due to the model definition as it was explained in the previous section. An important observation is that in contrast to the tensile the fibre stress profile is quite asymmetric around the fibre break. This is due to the fibre bending as the fibre fragments slide past each other after the onset of fibre failure (see Fig. 6(b)). These results also suggests that one-dimensional analyses such as shear-lag models would fail to accurately capture the mechanics of the problem as it is clear that this fibre failure mode causes also geometrical non-linearities. This fibre failure mode in compression induces high shear stresses in the surrounding matrix. The resulted shear stress field can be seen in Fig. 6(a). The shear stresses mainly change in the direction transverse to the fibre through the matrix material.

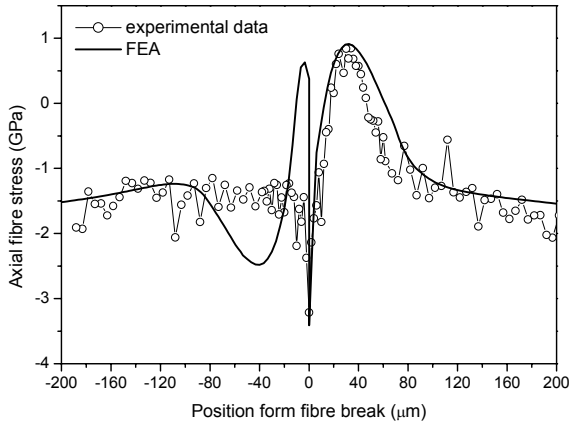

Fig. 5. Axial fibre stress in the vicinity of a compressive fibre break (x=0μm). The applied strain is –0.55%, and the coefficient of friction between the fibre fragments is 0.4.

Above the compressive behaviour of the single-fibre composites was reported in brief. The next step was to investigate the compressive behaviour of the multi-fibre composites (a bundle of fibres embedded in the epoxy matrix). As it was mentioned in the previous section the fibre stresses measured at different applied strains within a pre-selected area in the bundle of fibres. A histogram of the fibre strain values obtained from the mapping of a stress-free specimen is shown in Fig. 7. In the same graph, a histogram of the fibre strain values obtained from the same specimen strained at –0.5% is also given. As it can be seen, the fibre strains at an applied strain of –0.5% are considerably spread, as compared to the values for the unstrained case (residual strains). This spread on fibre strain distribution is indicative of the presence of a complex internal stress field. The obtained histograms were then converted to Gaussian distributions as a first approximation of the corresponding sets of measurements. In Fig. 8 the corresponding mean fibre strain value is plotted as a function of the applied strain

measured by means of the attached strain gauges. As can be seen, the mean value of the fibre strain distribution follows the 1:1 line up to an applied compressive strain of about –0.3%.

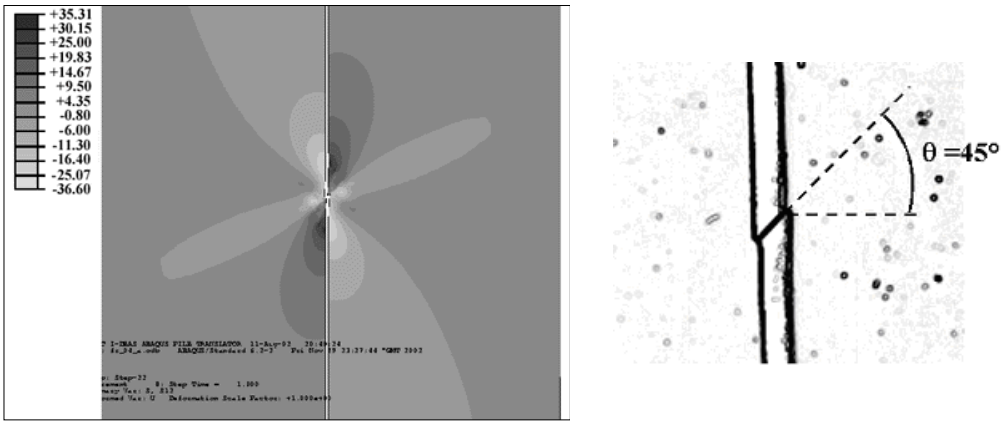

(a) (b)

Fig. 6. a) Shear stress field around the compressive fibre break at an of applied strain -0.55% (introduction of the fibre break). The coefficient of friction between the fibre fragments is 0.4 (all values in MPa), b) Micrograph of a typical compression induced shear fibre break,

This deviation from linearity is probably associated with the non-linear response of the carbon fibres themselves, which behave in a non-linear manner at strains higher to –0.35% approximately as it is shown in Fig. 3. In Fig. 8 the far-field strain values of a single-(discontinuous) fibre model composite [9] as a function of the applied strain is also given. In both cases: a) single and b) multi-fibre model composites a similar trend exists. This is accordance with the assumption made previously correlating the observed non-linearity with the non-linear behaviour of the high-modulus carbon fibres themselves. Furthermore it should be noted that up to an applied strain of –0.5% no fibre fractures were observed within the examined volume.

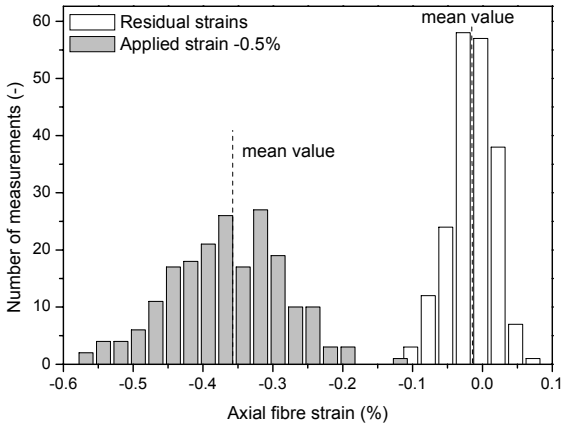

Fig. 7. Axial fibre strain histograms (number of measurements at each applied strain level, N=200).

Although no strain concentration factors were experimentally identified in the neighbourhood of fibre discontinuities (fibre ends) existing within the bundle of fibres, the failure process in these model composites suggests that indeed there is fibre-fibre interaction. Failure was sudden at an applied strain of –0.6% approximately. A typical failure mode for these multi-fibre microcomposites is shown in Fig. 9(a), where it can be seen that the fibres have failed in shear at a certain plane, whereas no fibre fractures have been observed far from the fracture planes. The way these fibres have failed is better shown in Fig. 9(b), where some typical shear induced fibre breaks can be seen. In all the experiments performed the fracture plane formed

an angle of about 18^o with the horizontal (see Fig. 9), furthermore 2-3 distinct fractures planes were identified per specimen.

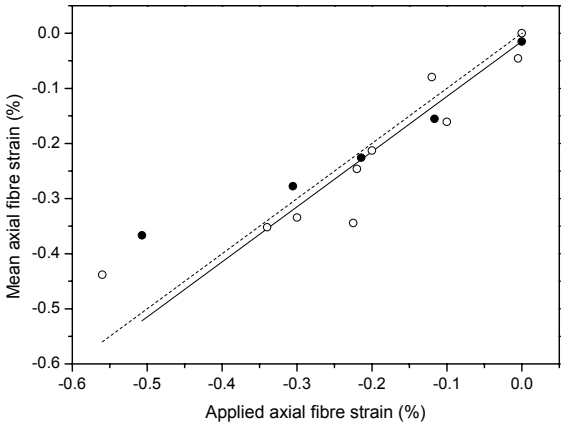

Fig. 8. ● Mean axial fibre strain (Raman measurements) as a function of the applied strain (strain gauges measurements) for the multi-fibre model composites (Fig. 1(a)). ○ Axial far-field fibre strain versus applied strain for single (discontinuous) fibre model composites [24].

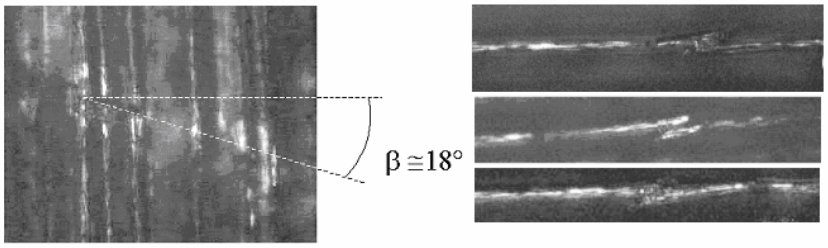

(a) (b)

Fig. 9. a) Optical micrograph of the fracture site showing fibres failed in shear in a bundle microcomposite (Fig. 1(b)), and b) Optical micrographs of shear induced fibre breaks under compressive loading taken from the fracture site of (a).

In order to further examine the existence of SCF's in the vicinity of fibre discontinuities (fibre ends) the FE method was employed. A similar model (consisting of 5 fibres and the inter-fibre spacing was one fibre diameter) to that one depicted in Fig. 4 was used. In order to model a fibre end the angle between the fibre fragments was changed from 45^o to 0^o. The FE analyses revealed that SCF's exist in the neighbouring fibres.

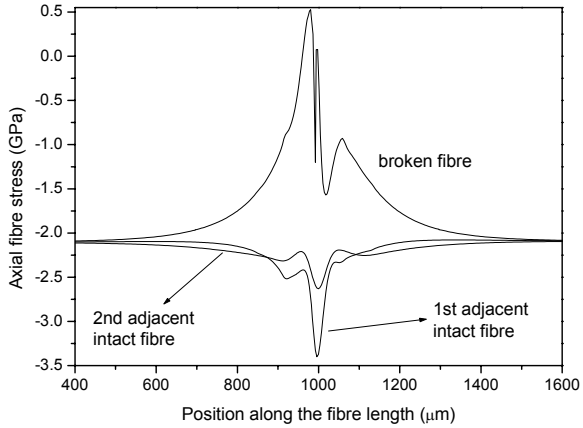

Fig. 10. Axial fibre stress profiles for the broken fibre and its adjacent intact fibres at an applied strain of –0.55%.

Then the angle between the fibre fragments was set to 45^o to simulate the effect of a compressive fibre break in the adjacent fibres. The results are depicted in Fig. 10 where the axial fibre stress was plotted for the broken fibre and the 1st and 2nd adjacent fibres at an applied strain of -0.55% (fibre break introduction). Another interesting observation is that in accordance with the experimental data of Goutianos et al. [9], the axial fibre stress in the broken fibre can have even positive (tensile) values due to fibre bending as the fibre fragments slide past each other. The predicted stress concentration factor for the first adjacent fibre is 1.62 and for the second fibre is 1.23. More importantly the position of these stress concentration factors lies at an angle, θ (see Fig. 11), of about 11.6^o at an applied strain of -0.55% (fibre break introduction). As the applied load increases the fibre fragments continuously slide past each other, which in turn result in an increase of angle θ. At an applied strain of -0.65% θ is about 14^o, which is reasonably close to the observed value of 18^o (see Figs. 9) taking into account the simplifications of the model.

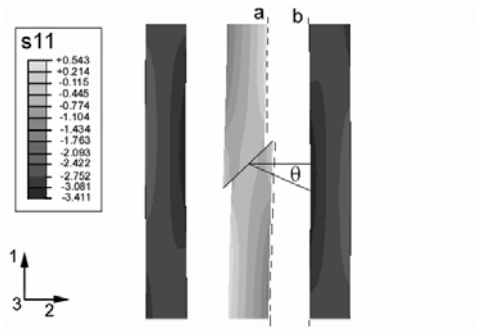

Fig. 11. Axial fibre stresses for the broken fibre (middle fibre) and its two first adjacent fibres at an applied strain of -0.55%. (All values in GPa).

As it has been mentioned above, it is widely believed that the compressive failure of unidirectional composites is controlled by the misalignment of the fibres. Due to this eccentricity the fibres easily buckle upon the application of a compressive load and this is the nucleation of a kink band which is then followed by its steady-state propagation. On the other hand in all the experiments performed during this work (including both single and multi-fibre model geometries) high modulus carbon fibres fail in shear and do not buckle. Even this mode of failure could result in kink band formation in unidirectional composites. The problem that arises is when failure starts in a composite. Obviously, if all the fibres in a composite are perfectly aligned to the loading axis then there is no preferential location where the first broken fibres appear if we assume that the fibre strength distribution in compression is quite small compared to the tensile case [10].

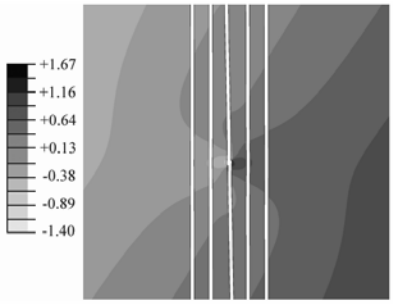

Fig. 12. Matrix transverse displacements at an applied strain of -0.55%. The misalignment of the central (broken fibre) is 1.5^o (all values in mm).

It has been shown that defects such as fibre ends could cause stress raisers in the adjacent intact fibres causing them to fail. In this way the nucleus of compressive failure could be formed, which then grows in an unstable manner. Another possible defect could be misaligned fibres, which obviously would fail before the straight fibres within the composite

volume. The FE model of Fig. 4 was modified to study the effect of a misaligned fibre. The model consisted of 5 fibres were the central fibre (where the fibre break is introduced) ha a misorientation angle of 1.5^o with respect to the loading axis and the inter-fibre spacing is four fibre diameters.

Fig. 12 shows the contour of the matrix transverse displacements after the fibre break introduction in the misaligned fibre. It can be observed that in this case the response of the composite is quite unstable due to the eccentricity created from the misaligned of the broken fibre. Of course this effect would be even more pronounced in the case of a region of misaligned fibres in a real composite, which would result in an unstable failure of mode.

Fig. 13 depicts the fibre stress in the broken and the 1st adjacent fibre for two different matrix yield stresses. It can be seen the matrix shear properties have an effect on the failure process. This is better seen in Fig. 13(b) where it can be seen that a change in the matrix yield stress result in a shift of the position of maximum stress in the adjacent fibre.

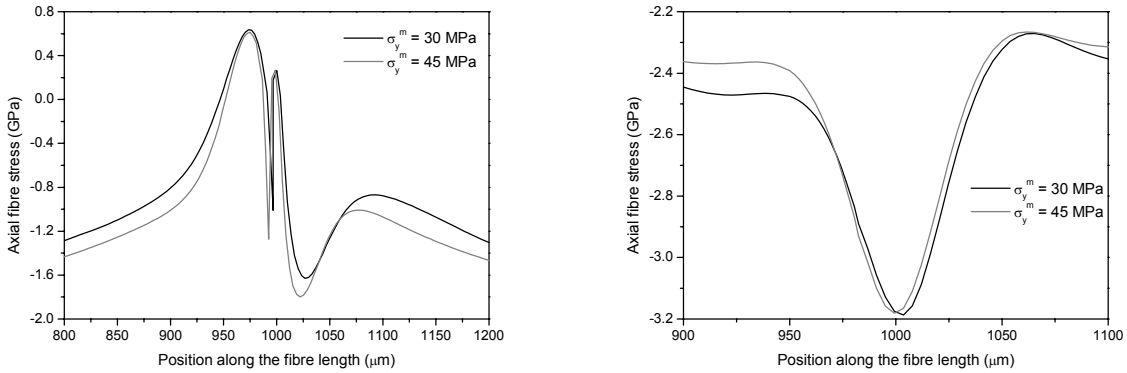

(a) (b)

Fig. 13. Axial fibre stress a) of the broken and b) of the first intact adjacent fibre for two different matrix yield stresses 30 and 45 MPa, respectively. The applied strain is -0.55% (introduction of the fibre break). The inter-fibre spacing is four fibre diameters and the broken fibre has a misorientation angle of 1.5^o with respect to the loading axis.

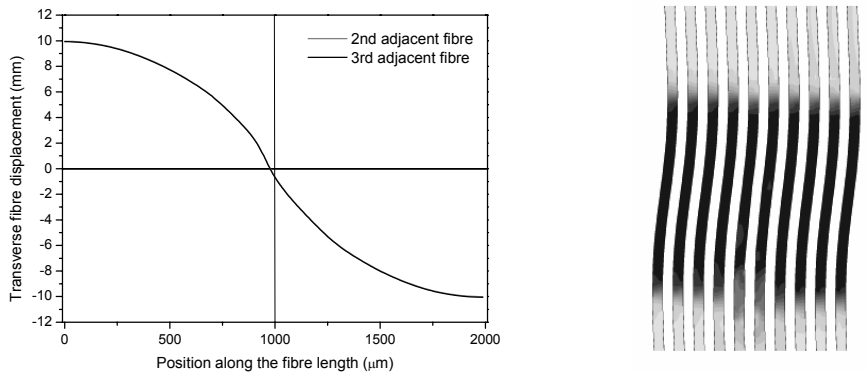

(a) (b)

Fig. 14. a) Transverse displacements of the 2nd and 3rd adjacent fibres to the broken fibre at an applied strain of -0.65%, b) Matrix shear stresses in the area near the fibre break in the planar array of 49 fibres (the fibre break position is at 1000μm.

Finally, the FE model of Fig. 4 was expanded in order to simulate the compressive behaviour a unidirectional lamina under compressive loading. The model now consists of 49 perfectly aligned. Similar to the cases presented above again the central fibre breaks at a certain applied strain, which in this case is -0.50%. Then by further increasing the applied strain the response of the composite is examined. The basic difference in the present model is that now the fibres are not surrounded by a huge amount of matrix and thus microbuckling is more likely to

occur. This can be seen in Fig. 14(a) where the transverse displacements of first two intact fibres are shown. Fig. 14(b) shows the deformed configuration of the array of fibres at an applied strain of -0.65% forming a kink band. The microbuckling of Fig 14(b) is caused by only one fibre break. In reality at this applied strain level more fibre breaks should have failed as shown above and as a result the final kink band would be more narrow and localised at a certain area.

5. CONCLUSIONS

In this work use it was shown that high-modulus carbon fibres fail in shear in compression. This failure mode results in a higher rate of stress transfer, and therefore the corresponding stress transfer length is smaller. At low strains an approximately linear relationship between fibre strain and applied strain is obtained. At high compressive strains a deviation from linearity is observed accompanied by a spread of fibre strain distributions. The failure mode experimentally observed, a plane of fractured fibres, suggests that there is fibre-fibre interaction. This is also supported by the FEA predictions, where a SCF was found in the adjacent fibres at a small angle with respect to the fibre break location. Far from the fracture area no fibre breaks were observed, the fibres remained aligned to the loading axis. Then the effect of fibre misalignment on the compressive behaviour was examined. A misoriented fibre was found to result in an unstable response after the fibre introduction. Finally, the compressive response of a unidirectional lamina investigated. The main finding was that even in a perfectly aligned lamina a compressive (shear) fibre break kink band formation could be predicted.

References

1. Berbineau, P., Soutis, C., Guz, I.Z., “Compressive failure of 00 unidirectional carbon-fibre-reinforced plastic (CFRP) laminates by fibre microbuckling”, *Comp Sci Technol*, **59** (1999), 1451-1455.
2. Rosen, B.W., “Mechanics of composite strengthening. Fibre Composite Materials”, American Society of Metals 1965, 37-75.
3. Schuerch, H., “Prediction of compressive strength in uniaxial boron fibre-metal composite materials”, *AIAA Journal*, **4** (1966), 102-106.
4. Budiansky, B., “Micromechanics”, *Comput* S*truct*, **16** (1983), 3-12.
5. Kozey, V.V., “Splitting-related kinking failure mode in unidirectional composites under compressive loading”, *J Mater Sci Lett*, **12** (1993), 43-47.
6. Lankford, J., “Compressive failure of fibre-reinforced composites: Buckling, kinking, and the role of the interface”, *J. Mater. Sci.*, **30** (1995), 4343–4348.
7. Narayanan, S., Schadler, L.S., “Mechanisms of kink-band formation in graphite/epoxy composites: a micromechanical experimental study”, *Comp Sci Technol*, **59** (1999), 2201-2213.
8. Garland, B.D., Beyerlein, I.J., Schadler, L.S., “The development of compression damage zones in fibrous composites”, *Comp Sci Technol*, **61** (2001), 2461-2480.
9. Goutianos, S., Peijs, T., Galiotis, C., “Mechanisms of stress transfer and interface integrity in carbon/epoxy composites under compression loading: Part I: Experimental investigation”, *International Journal of Solids and Structures*, **39** (2002), 3217-3231.
10. Nakatani, M., Shioya, M., Yamashita, J., “Axial compressive fracture of carbon fibres”, *Carbon* **37** (1999), 601-608.